RESOLUTION AND VISIBILITY ENHANCEMENT OF ULTRASONIC ECHOES REELECTED FROM TARGETS HIDDEN BY HIGHLY REVERBERANT THIN LAYERS

J. Saniie

Department of Electrical and Computer Engineering
Illinois Institute of Technology
Chicago, Illinois 60616

ABSTRACT

In the ultrasonic imaging of many materials, the measured signal consists of multiple echoes (reverberation) which complicate direct characterization of the target. In an earlier report [7] it has been shown that ultrasonic echo classification can facilitate imaging of targets hidden by highly reverberant thin layers. Among all classes of echoes, two sequences of multiple echoes have been found to be essential in target characterization. In this report we present several processing techniques developed for separating these sequences and enhancing the visibility of those echoes backscattered from the hidden target. Techniques used include substraction, correlation, spectrum and cepstrum analysis. The combination of these techniques enhances the signal-to-noise ratio and improves the resolution of the measurement. The mathematical model of the reverberation and experimental results will be presented. Experimental results are in close agreement with the mathematical model.

INTRODUCTION

Reverberation occurs in ultrasonic imaging of many materials [1-3,5] including in the thickness measurement of thin planar defects in metal, in lamination of composite bonds, in the gap thickness measurements of the metal adhesively bonded systems, oil film measurements, fatigue crack analysis, etc.. In this report we present methods for unraveling the multiple echoes backscattered from highly reverberant layered structures. The emphasis of the present discussion is focused on the signal processing schemes useful in signal-to-noise ratio enhancement and improvement of resolution.

Consider the planar geometry of multiple thin Layers as shown in Figure 1. It is assumed that the ultrasonic transducer is positioned in Region I, and Region II is a highly reverberant thin layer. It is our objective to recognize echoes backscattered from region IV. The usefulness of this study becomes apparent when imaging targets which are hidden behind a reverberant thin layer. During a given scanning time the received signal is comprised of multiple echoes detected after traveling m times in Region II and n times in Region III,

$$r(t) = \sum_{m=0}^{\infty} \sum_{n=0}^{\infty} \gamma_{mn} u(t-2mT_2 - 2nT_3) \qquad (1)$$

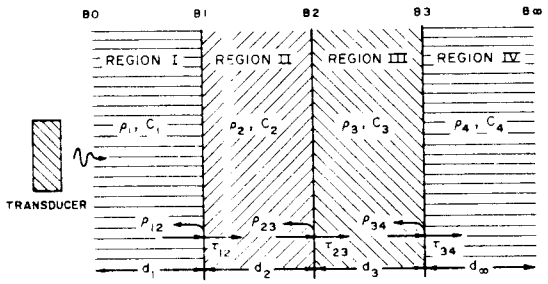

c_i : Velocity

ρ_i : Density

i, j = 1, 2, 3, 4

Fig. 1. Multilayer structure consisting of four different regions.

where u(t) represents the measuring system impusle response, T_2 represents traveling time in Region II, T_3 represents traveling time in Region III, and the term γ_{mn} is the received echo amplitude related to the reflection coefficient, ρ_{ij}, or the transmission coefficient, τ_{ij}. It is assumed that the incident wave is normal to the boundaries of the layers, and for the sake of simplifying mathematical development, the effects of attenuation and measurement noise are ignored.

After a given time many echoes which have traveled through the layered structure following different paths of reverberation can be detected. Discrimination of these traveling waves is quite complicated. In order to better understand the nature of the received echoes, we have extended our work to computer simulation and wave classification [6-8].

WAVE CLASSIFICATION

After considerable experimentation and computer simulation, an appropriate identification and classification, technique was developed which allowed characterization of the layered structure of those detected echoes of significant intensities [6]. As a result of classification, the generalized model for received echoes given in equation (1) can be presented differently,

$$r(t) = \rho_{12} u(t) + \sum_{k=1}^{\infty} a_k u(t-2kT_2) + \sum_{k=1}^{\infty} b_k u(t-2T_3-2kT_2)$$
$$+ \sum_{k=1}^{\infty} c_k u(t-4T_3-2kT_2) + \sum_{k=1}^{\infty} d_k u(t-6T_3-2kT_2) + \cdots \qquad (2)$$

0090-5607/84/0000-0903 $1.00 © 1984 IEEE

where a_k is the amplitude of class 'a' echoes which reverberate continually in Region II only; b_k is the amplitude of class 'b' echoes which reverberate continually in Region II, and once in Region III; c_k is the amplitude of class 'c' echoes which reverberate continually in Region II, and twice in Region III; etc..

Of all classes of echoes which are detected from reverberant targets, class 'a' and 'b' echoes are the most dominant [6]. The amplitude of class 'a' echoes can be expressed as

$$a_k = \tau_{12}\,\tau_{21}\,\rho_{21}^{k-1}\,\rho_{23}^{k} \,. \qquad (3)$$

Since $|\rho_{21}|$ and $|\rho_{23}|$ are less than unity, the magnitude of type 'a' echoes decreases as the number of reverberation echoes, k, increases. According to the class 'b' definition the values of 'b' echoes are [6]

$$b_k = k\tau_{12}\,\tau_{21}\,\tau_{23}\,\tau_{32}\,\rho_{34}\,\rho_{21}^{k-1}\,\rho_{23}^{k-1} \,. \qquad (4)$$

The evaluation of b_k in terms of k, and Regions I, II, III and IV is more involved. Envelopes of class 'b' echoes for various characteristic impedances of Region I-IV are shown in Figure 2(a-d). Figures 2a-2d show instances of severe to mild reverberation in Region II. In each Figure, Graphs I-IV represent insignificant to significant acoustical mismatch between Region III and Region IV. The maximum of class 'b' echoes in terms of reverberation number k can be calculated by setting $\delta b_k/\delta k = 0$,

$$k = \frac{-1}{\log_e(\rho_{21}\rho_{23})} \,, \quad \text{integer k.} \qquad (5)$$

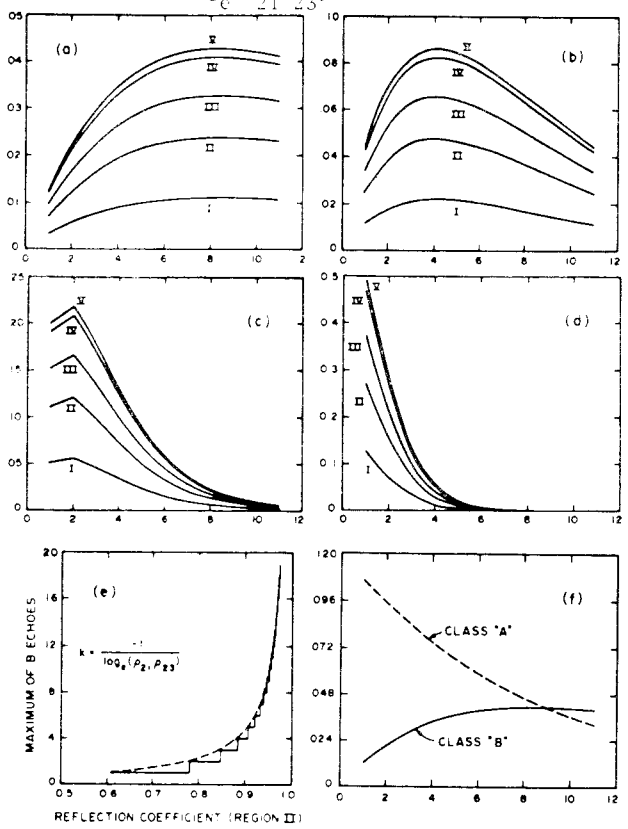

Fig. 2. Evaluation of class 'a' and 'b' echoes.

Graphical presentation of the maximum of class 'b' echoes as a function of $(\rho_{21}\rho_{23})^{1/2}$ is shown in Figure 2e. The severe mismatch between the characteristic impedances of Regions II and I, and Regions II and III, results in prolonged reverberation. In other words, the 'b' echoes will increase in amplitude with time, and thus, become more visible, while class 'a' amplitude decreases. Note that this is only true for highly reverberant layered targets.

These graphical results are very useful in the interpretation of the received signal which leads to the determination of the best region in time for class 'b' echo evaluation. For example, the best region for evaluating the echoes from a highly reverberant layered structure consisting of water, Inconel thin layer, water, and steel plate is near b_8 (see Fig. 2f for the comparison of the envelope of the class 'a' and 'b' echoes).

For further verification of the proposed classification technique, a computer program was developed to simulate the output of a pulse-echo ultrasonic system [6]. Figure 3 shows simulated A-scans of a structure composed of four regions: water, Inconel layer, water, and steel plate. In this figure each class of echoes has a unique arrival time and the 'b' type echoes can be seen growing with respect to the type 'a' echoes. The presence of class 'c' echoes is apparent, although their amplitudes are smaller than class 'a' and class 'b' echoes. For a whole range of applications significant interference can be expected among all classes of echoes. Therefore, additional signal processing is necessary for decoupling these classes of echoes.

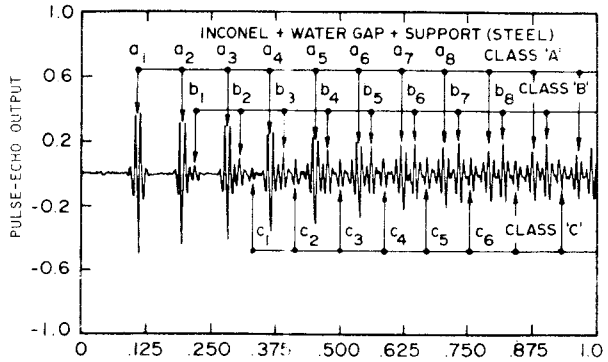

Fig. 3. Computer simulations of an A-scan of highly reverberant structure.

DECOMPOSITION OF MULTIPLE ECHOES

The major purpose of signal processing in this study is to decompose the backscattered signals and to distinguish the class 'a' and 'b' echoes. Without separating these echoes, imaging of a target through highly reverberant thin layers is difficult.

Equation (2) represents the classified backscattered signal in general. However, in the digital processing of the measured signal, we deal with a segmented portion of the reverberant echoes. This can be modeled as

$$\tilde{r}(t) = s_1(t) + s_2(t - 2T_3) + n(t) \qquad (6)$$

where

$$s_1(t) = \sum_{k=L}^{N} a_k u(t - 2kT_2)$$

$$s_2(t) = \sum_{k=L}^{N} b_k u(t - 2kT_2) \qquad (7)$$

$$2L\,T_2 < t < 2\,N\,T_2 + 2T_3$$

$n(t)$ = All other echoes plus measurement noise.

The selection of L and N must be such that the intensity of class 'b' echoes are larger or at least comparable to class 'a' echoes and, in addition, the noise n(t) is insignificant.

The signal $\tilde{r}(t)$ can be viewed as the sum of two sequences of multiple echoes each has a period of $2T_2$, and a delay of $2T_3$. In distinction of these two sequences of multiple echoes, the best situation arises when

$$T_3 = (K+\Delta)T_2 \quad ; \quad K = 0, 1, 2, \cdots$$
$$\Delta = 1/2. \qquad (8)$$

However, in general, Δ can be any value between zero and one. This means $s_1(t)$ and $s_2(t)$ may interfer significantly and, consequently, signal processing for wave decomposition and/or improvement of the system resolution becomes essential. Furthermore, existence of n(t) demands signal processing for signal-to-noise ratio enhancement. Digital signal processing used in the present report includes subtraction, correlation, spectrum and cepstrum analysis.

Substraction Method

Direct wave decomposition can be achieved by a simple subtraction scheme. Experimental verification of our classification technique and its usefulness is investigated in the multilayer structure shown in Figure 1. The four regions consist of water, Inconel layer (56 mils), water and steel plate. The transducer used in this measurement has approximately a 15 MHz center frequency, and the signal is digitized at 100 MHz. The digitized data has poor signal-to-noise ratio, due to the uncertainty in the timing of the sampling interval, especially when operating at 100 MHz. However, by incorporating a coherent averaging technique, the signal-to-noise ratio of the measured signal was improved significantly.

Experimental results are shown in Figure 4. The uppermost A-scan in this figure shows the reverberation echoes produced by the 56 mil thick flat Inconel layer, suspended in a water bath. As expected, the uniformly spaced class 'a' echoes decrease with time as energy leaks from the reverberating wave packet into the surrounding water bath. The center trace shows the effect of positioning a steel plate behind the Inconel in such a way that it leaves a water gap of approximately 10 mils. Although the addition of the support plate introduces both class 'b' and 'c' type echoes, their exact location is not easily resolved. By subtracting the reference signal (upper trace) from the A-scan of the multilayer structure (center trace), the class 'a' signals can be removed, clearly revealing the locations of the class 'b' and 'c' echoes. The bottom trace of Figure 4 shows the result of this simple processing. In this trace, the inverted 'b' type echoes are easily identified and show the characteristic increase in amplitude with increasing time. Finally the water gap width is determined from the measured delay between a type 'a' echo and its associated type 'b' echo as shown in the figure.

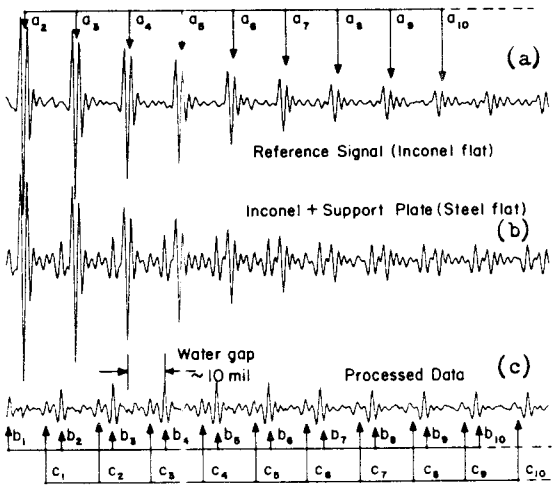

Fig. 4. Experimental measurement of reverberation. (a) Multiple echoes backscattered from a thin layer structure (class 'a' echoes). (b) Multiple echoes backscattered from a multilayer structure (class 'a', class 'b', etc.). (c) Subtraction results.

Correlation Method

An alternative method for obtaining the amplitudes and arrival times of composite signals is to use the amplitude and location of the peaks in the matched filter output. It has been shown [6], that maximal signal-to-noise (SNR) enhancement can be obtained when the class 'a' echoes are used as a matched function for performing circular autocorrelation. Numerical implementation of circular correlations is accomplished by utilizing the fast Fourier transform (FFT).

In order to evaluate the performance of the correlation functions, we first measure signals from a thin layer and a multilayer structure as shown in Figures 5-I and 5-II. The autocorrelation of the thin layer signal is normalized to ±1 and the maximum of the correlation function is circularly shifted to the center of the plot (see Fig. 5-III). The SNR enhancement achieved in the correlation output is apparent. In particular, a few spurious echoes after the first and second echo (see Fig. 5-I) have been significantly suppressed in the correlation output shown in Fig. 5-III). The cross-correlation of the thin layer and multilayer signals is presented in Fig. 5-IV. In this figure the class 'b' echoes are enhanced as well as the class 'a' echoes.

The matched filter approach for estimating the desired parameters is appealing because of the ease with which it can be implemented, especially in the

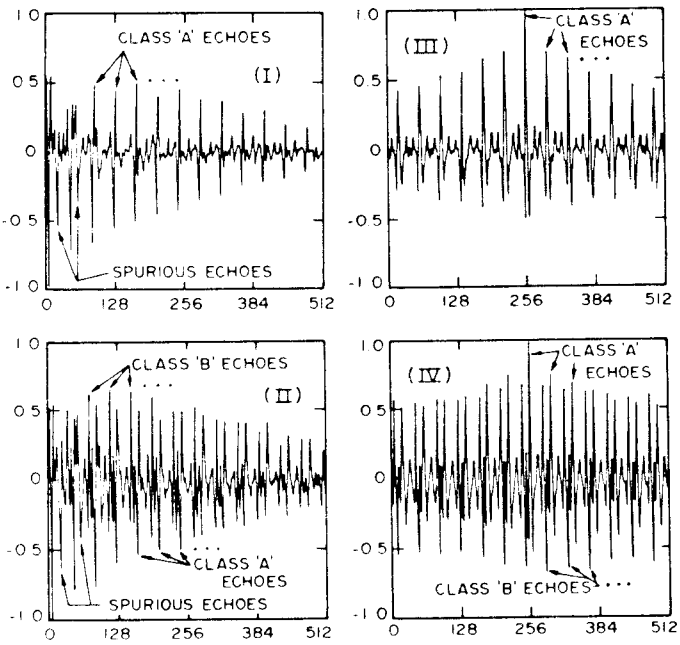

Fig. 5. Signal-to-noise ratio enhancement by correlation technique. Spurious echoes as marked in Figs. I and II are suppressed significantly in autocorrelation of class 'a' echoes, Fig. III, and cross-correlation of class 'a' and class 'b' echoes, Fig. IV.

case where individual signals are separated by times greater than the duration of the signal autocorrelation function. Unfortunately, in many cases of interest, the signal separation is less than the duration of the autocorrelation function of the signal; and thus the matched filter outputs for the individual echoes overlap. For this reason, matched filter processing alone is usually not sufficient for obtaining an accurate estimate of amplitudes and arrival times for closely spaced multipath targets.

Spectrum and Cepstrum Method

Transformation generally results in the simplification of the solution and analysis of a problem. In analyzing reverberant echoes, both power spectrum and cepstrum contain features which can be related to class 'a' and class 'b' echoes.

The Fourier transform of $\tilde{r}(t)$ is

$$\tilde{R}(\omega) = S_1(\omega) + S_2(\omega)e^{-2j\omega T_3} + N(\omega). \quad (9)$$

The power spectrum of class 'a' or class 'b' echoes consists of peaks separated by constant frequency spacing as shown in Figures 6a-6d. It can be shown that the frequency differences between consecutive peaks is inversely proportional to T_2 [6]. However, the power spectrum of $|\tilde{R}(\omega)|^2$ cannot directly be related to the delay between class 'a' and class 'b' echoes. Furthermore, no specific pattern can be found which describes the intensity of class 'b' echoes needed for characterizing the hidden target.

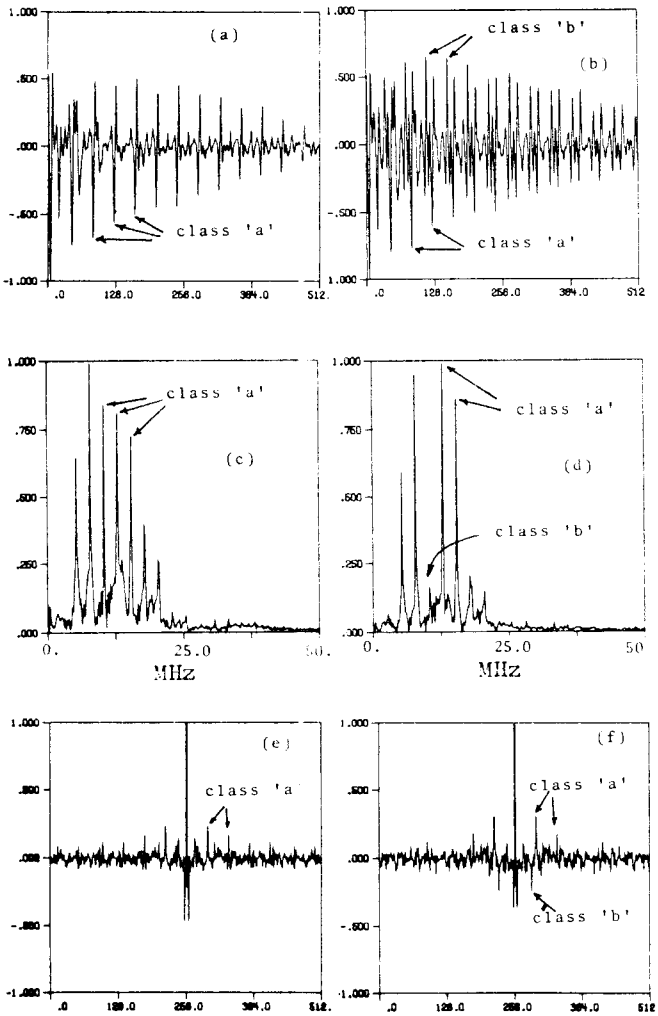

Fig. 6. Power spectrum and cepstrum results of reverberant echoes. (a) Signal of a thin layer, (b) signal of a multilayer structure, (c) power spectrum of signal in (a), (d) power spectrum of signal in (b), (e) power cepstrum of signal in (a), and (f) power cepstrum of signal in (b).

Homomorphic analysis (also referred to cepstrum analysis) has been used in speech and seismic data analysis for dereverberation [4]. In this study, homomorphic processing is potentially useful in decomposing class 'a' and class 'b' echoes. In particular, the power cepstrum (defined as the inverse Fourier Transform of the log of the power spectrum, $F^{-1}[\log|\tilde{R}(\omega)|^2]$) of reverberant echoes appears to be effective in displaying the presence and intensity of class 'b' echoes [6]. Experimental results of power cepstrum are shown in Figures 6e and 6f. A special case occurs when class 'a'

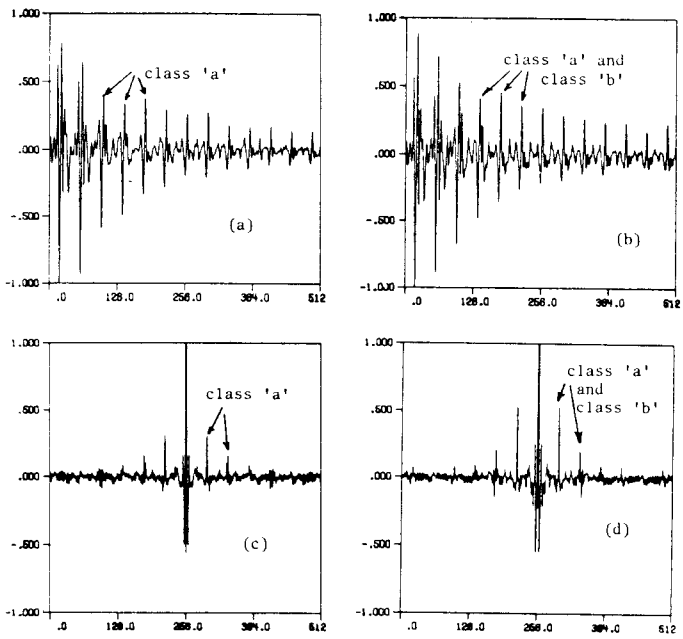

Fig. 7. Power cepstrum results of a reverberant backscattered signal when class 'a' and class 'b' echoes are superimposed. (a) Signal of a thin layer, (b) signal of a multilayer structure, (c) power cepstrum of signal in (a), and (d) power cepstrum of signal in (b).

and class 'b' are superimposed, as shown in Figure 7. Comparison of a thin layer signal (see Figure 7a) and the multilayer signal (see Figure 7b) indicate minor differences in the time signal. However, the differences are more pronounced in their corresponding power cepstrum (see Figures 7c and 7d).

CONCLUSION

This report has dealt with the development and evaluation of the digital signal processing techniques in imaging targets hidden by highly reverberant thin layers. Two sequences of multiple echoes have been found to be essential in target characterization. Digital processing techniques such as subtraction, correlation, spectrum and cepstrum analysis are used in order to enhance the resolution and visibility of ultrasonic echoes reflected from hidden targets. Subtraction has been found to be effective in removing undesired echoes. Correlation improves the signal-to-noise ratio at a moderate degradation of resolution. The power spectrum of the backscattered echoes is affected by the presence of the hidden target's echoes, although no specific pattern can be found. The power cepstrum exhibits strong impulses of narrow duration related to the echoes backscattered from the hidden target. The combination of these digital signal processing techniques enhance the detection and characterization of target hidden by highly reverberant thin layers.

REFERENCES

[1] H.H. Chaskelis and A.V. Clark, "Ultrasonic Nondestructive Bond Evaluation: An Analysis of the Problem", Materials Evaluation, Vol. 38, pp. 20-38 (1980).

[2] J. Krautkramer, Ultrasonic Testing of Materials, Springer-Verlag, New York (1975).

[3] S. Lees, "Ultrasonic Measurement of Thin Layers", IEEE Trans. Sonics and Ultrasonics, Vol. SU-18, No. 2, pp. 81-88 (1971).

[4] A.V. Oppenheim and R.W. Schafer, Digital Signal Processing, Prentice-Hall, Inc., Princeton, NJ, (1975).

[5] J.L. Rose and P.A. Meyer, "Ultrasound Signal Processing Concepts for Measuring the Thickness of Thin Layers", Materials Evaluation, Vol. 32, pp. 249-255 (1974).

[6] J. Saniie, "Ultrasonic Signal Processing: System Identification and Parameter Estimation of Reverberant and Inhomogeneous Targets", Ph.D. Thesis, Purdue University (1981).

[7] J. Saniie, E.S. Furgason, and V.L. Newhouse, "Ultrasonic Imaging Through Highly Reverberant Thin Layers - Theoretical Considerations", Materials Evaluation. Vol. 40, pp. 115-121 (1982).

[8] J. Saniie, "Identification of Reverberant Layered Targets Through Ultrasonic Wave Classification", Review of Progress in Quantitative Nondestructive Evaluation, Eds.: D.O. Thompson and D.E. Chimenti, Plenum Press, pp. 1011-1018 (1984).